



This is a repository copy of *Open-Circuit Voltage in Inverted Polycarbazole:Fullerene Bulk Heterojunction Solar Cells*.

White Rose Research Online URL for this paper:  
<http://eprints.whiterose.ac.uk/104230/>

Version: Accepted Version

---

**Article:**

Alqurashi, R., Griffin, J., Alsulami, A. et al. (1 more author) (2016) Open-Circuit Voltage in Inverted Polycarbazole:Fullerene Bulk Heterojunction Solar Cells. *IEEE Journal of Photovoltaics*, 6 (4). pp. 918-923. ISSN 2156-3381

<https://doi.org/10.1109/JPHOTOV.2016.2553850>

---

**Reuse**

Unless indicated otherwise, fulltext items are protected by copyright with all rights reserved. The copyright exception in section 29 of the Copyright, Designs and Patents Act 1988 allows the making of a single copy solely for the purpose of non-commercial research or private study within the limits of fair dealing. The publisher or other rights-holder may allow further reproduction and re-use of this version - refer to the White Rose Research Online record for this item. Where records identify the publisher as the copyright holder, users can verify any specific terms of use on the publisher's website.

**Takedown**

If you consider content in White Rose Research Online to be in breach of UK law, please notify us by emailing [eprints@whiterose.ac.uk](mailto:eprints@whiterose.ac.uk) including the URL of the record and the reason for the withdrawal request.



[eprints@whiterose.ac.uk](mailto:eprints@whiterose.ac.uk)  
<https://eprints.whiterose.ac.uk/>

# Open-circuit Voltage in Inverted Polycarbazole: Fullerene Bulk Heterojunction Solar Cells

Rania Alqurashi<sup>1</sup>, Jonathan Griffin<sup>1</sup>, Abdullah Alsulami<sup>1</sup>, Alastair Buckley<sup>1</sup>

<sup>1</sup> Department of Physics and Astronomy, University of Sheffield, Hicks Building, Hounsfield Street, S3 7RH, UK

## ABSTRACT

The correlation between cathode work function and open-circuit voltages ( $V_{oc}$ ) in inverted polycarbazole: fullerene (PCDTBT: PC<sub>70</sub>BM) bulk-heterojunction solar cells has been investigated by post-annealing of tin-indium oxide (ITO) electrodes. ITO work function is seen to change from 4.2 eV to 4.5 eV without the need to insert additional interfacial layers with annealing temperature up to 400°C. The best device performance was obtained at room temperature with ITO work function of 4.2 eV with  $V_{oc}$  of 0.89 eV,  $J_{sc}$  of 8.06 mA.cm<sup>-2</sup>, FF of 64.70 % and PCE of 4.62 %. Together with previously published results, we are able to extract two regimes of  $V_{oc}$  dependence on cathode work function. First, a linear relationship when the cathode work function exceeds the lowest unoccupied molecular orbital (LUMO) of PCBM and second a constant  $V_{oc}$  regime when the ITO work function reduces below the LUMO level. These results provide general guidelines for cathode contact design in inverted polymer solar cells.

## 1. Introduction

Polymer solar cells (PSCs) are an attractive class of next-generation photovoltaics, because they are mechanically flexible, lightweight, and compatible for roll-to-roll fabrication [1]. A high power conversion efficiency (PCE) exceeding 10 % has recently been reported for single-junction inverted polymer solar cells [2]. Indeed, the majority of highly efficient PSCs certified and reported to date are employing narrow-bandgap polymer donors as well as an inverted structure, in which an indium-tin oxide (ITO) bottom-electrode serves as an electron collector. While narrow-bandgap polymer donors enhance the photocurrent generation [3], the inverted structure has advantages compared to the standard structure in terms of device stability [4] and manufacturability [5]. However, tuning the ITO work function (WF) to minimize the mismatch with the lowest unoccupied molecular orbital (LUMO) energy level of the acceptor molecules remains a great challenge for fabricating highly efficient PSCs. This is because the overall PCE is dependent on the open-circuit voltage ( $V_{oc}$ ). Understanding the correlation between the electronic structure of ITO and  $V_{oc}$  is extremely beneficial in device engineering and contact design.

At the open circuit condition, a potential difference between the anode and cathode electrodes forms as a result of the accumulation of free-photogenerated carriers [6]. It outweighs the built-in potential by equalizing the generation and recombination currents. Hence, the system reaches a quasi-equilibrium state, and the  $V_{oc}$  is defined by the potential difference formed. However, early works have reported the weak dependence of  $V_{oc}$  on the work function of particular electrodes when an ohmic contact forms. It is instead influenced by other factors; the acceptor strength [7], light intensity [8], processing conditions of the blend layer [9][10], donor oxidation potential [11], and temperature [12]. This is mainly attributed to the observation of Fermi level pinning across the interface. Taking into account those factors, a new  $V_{oc}$  definition has been proposed by Sacarber et al [13], who correlate the open circuit voltage to the donor-acceptor band gap ( $E_g$ ) dictated by the energy onset between the HOMO level of polymer donors and the LUMO level of acceptor molecules.

The origin of Fermi level pinning is explained through integer charge transfer (ICT) [14][15] between the electrode and the organic material. In the ICT model the Fermi level pins when the electrode work function exceeds the polaronic energy level of polymer donors, facilitated by spontaneous charge transfer into empty states near the interface. This integer charge transfer leads to the formation of an interfacial dipole layer [16][17]. An implication of the charge transfer at both the anode and cathode interfaces can be a loss in the achievable  $V_{oc}$  [18][19] due to the induced trap-assisted recombination [20]. The energetic disorder that arises from the weak-ground states interaction between the polymer donor and acceptor molecules within the bulk heterojunction layer can also affect  $V_{oc}$  [15][17][21]. Furthermore, the degree of disorder in the blend film influences the amount of voltage loss, in which the splitting of the electron and hole Fermi levels is reduced by restricting the accumulation of carries into the tails of the density of states [22], giving rise to the radiative recombination [19].

In the case of non-ohmic contact, the vacuum level regulates the energy level alignment and  $V_{oc}$  is determined by the difference between electrodes work function [23][16]. There will be no charge transfer, and the energy level alignment across the interface follows the Schottky-Mott limit [17]. Consequently,  $V_{oc}$  becomes sensitive to the height barrier for charge extraction. Note that so far, the majority of progress made in understanding the origin of  $V_{oc}$  in polymer solar cells has considered only hole extraction. Our work investigates the changes in ITO work function with the open circuit voltage of inverted polymer solar cells considering the electron extraction.

In this work, we are able to tune the open-circuit voltages of inverted PSCs based on poly(N-9'-heptadecanyl-2-7-carbazole-alt-5,5-(4',7'-di-2-thienyl-2'-1'-3'-benzothiadiazole) (PCDTBT) and [6,6]-phenyl-C<sub>71</sub> butyric acid methyl ester (PC<sub>70</sub>BM) blended heterojunction (BHJ), by thermal annealing of ITO electrodes with no interfacial layer inserted. The best device performance was obtained at room temperature;  $V_{oc}$  of 0.89 eV,  $J_{sc}$  of 8.06 mA.cm<sup>-2</sup>, FF of 64.70 % and PCE of 4.62 %. Ultraviolet photoelectron spectroscopy (UPS) and x-ray photoelectron spectroscopy (XPS) studies justify the increase in ITO work function by 0.3 eV upon annealing is a result of the induced metallic defect states.

## 2. Experimental

### 2.1. Materials

Indium-tin oxide (ITO) coated glass substrates with sheet resistance of 15 ohm/square were purchased from Ossila Ltd. The polymer donor PCDTBT and acceptor molecules PC<sub>70</sub>BM were provided by Ossila Ltd and used as received.

### 2.2. Device Fabrication and Characterization

A schematic of device configuration of inverted PCDTBT: PC<sub>70</sub>BM solar cells reported here is shown in Figure 1(a). However, pre-patterned ITO coated substrates were sequentially cleaned in a hot water bath of various detergents; Hellmanex, deionized water and isopropanol for 10 m each and blow-dried under nitrogen flow. The pre-cleaned substrates were annealed at range of temperatures up to 400°C in air. The blend solution of PCDTBT: PC<sub>70</sub>BM (1:4 wt %) prepared in chlorobenzene was spin-coated directly onto ITO electrodes. The blend film (90 nm) was dried at 80 °C for 15 m. Then, the top anode contacts of MoO<sub>3</sub> (20 nm) and Al (100 nm) layers were thermally evaporated in a vacuum chamber (10<sup>-7</sup> Pa), respectively. The current density- voltage (JV) characteristics of the cells were measured

in ambient under the illumination of a simulated solar light with  $100 \text{ mW.cm}^{-2}$  (AM1.5) using a solar simulator (Keithley, 92251A-1000). All measurements were undertaken at room temperature.

### 2.3. Interfacial Characterization

The UPS and XPS measurements were performed under ultrahigh vacuum using a Kratos ultra AXIS photoelectron spectrometer. He I emission line (21.22 eV) and monochromatic Al K  $\alpha$  line (1486.6 eV) were used as excitation sources for UPS and XPS, respectively. All UPS spectra were recorded at normal emission angle under room temperature. Vacuum level shifts were determined from UPS spectra at low-Kinetic energy onset (secondary electron cut off) with -9 sample bias. The sample preparation for UPS/XPS measurements followed the same procedure for device fabrication.

## 3. Results and discussion

Figure 1(b) illustrates the photovoltaic characteristics of inverted PCDTBT: PC<sub>70</sub>BM solar cells upon annealing of ITO electrodes. The devices exhibit generally good JV curves with no S-shaped kinks even when the annealing temperature increases. It is known that the appearance of S-shaped kinks are the result of interface degradation at cathode-polymer interfaces [24], formation of dipole interfacial [25], height barrier for hole injection [26], and surface recombination velocity of majority charge carriers [27]. However, the absence of this deformation confirms the good quality of diode characteristics obtained, which is reported here for the first time. Indeed, ITO only devices reported in literature for inverted BHJ PSCs previously show very poor performance [28][29][30][31]. An implication of this result is the sensitivity of ITO electrodes to the pre-treatment conditioning.

Furthermore, having no S-shaped kinks are crucial to distinguish the reason of lowering fill factor upon annealing (see S1 in the supporting information). The fill factor is known to be regulated by charge carrier transport and is given by  $FF = P_{\text{out}} / V_{\text{oc}} J_{\text{sc}}$ , where  $P_{\text{out}}$  is the maximum power delivered by the solar cell. A clear shift in JV curves towards low  $V_{\text{oc}}$  is observed with increasing annealing temperatures from 25 °C to 400 °C while only small changes are observed for  $J_{\text{sc}}$ . The reason of  $V_{\text{oc}}$  reduction will be discussed later on. However, a correlation between the short circuit current and series resistance was established as a function of ITO annealing (see S2 in the supporting information). The series resistance in our devices is a sum of ITO sheet resistance and interfacial resistances at both electrodes. We have made a quick experiment to measure the sheet resistance of annealed ITO using a multimeter. It has been found that ITO sheet resistance is somewhat constant for low temperatures up to 300 °C. At high temperatures from 300 °C to 400 °C, changes in ITO resistance are equivalent to a 20 % increase of the initial value, which is in an agreement with Bhatti et al. work [32]. They measured the sheet resistance of annealed ITO thin films by a four-point probe and explained the rise in the sheet resistance at temperatures  $\geq 300$  °C by the filling up of oxygen vacancies. An evidence of the introduction of defects upon annealing is seen in our XPS results and will be discussed in details later.

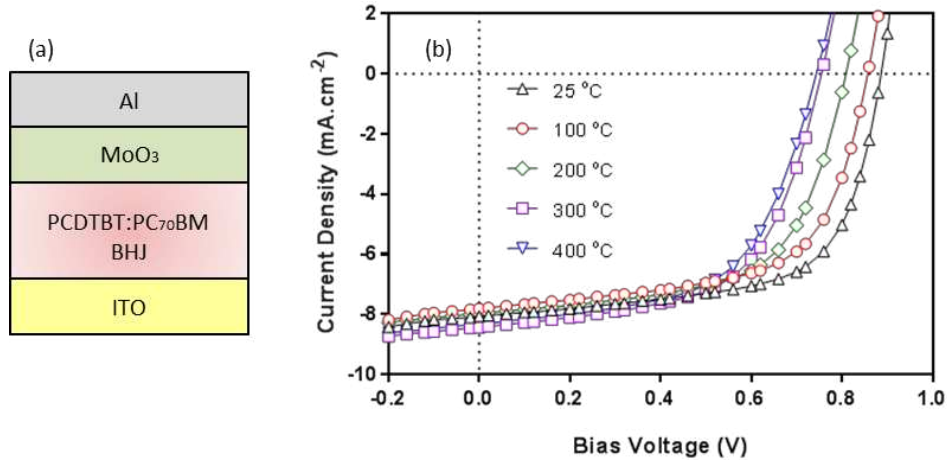


**FIG. 1.** (a) Typical device configuration of inverted solar cells with no cathode interfacial layers inserted. (b) Current density vs voltage (J-V) curves for inverted PCDTBT: PCBM devices as a function of ITO annealing temperatures.

**Table 1.** The average values of device parameters; open-circuit voltage, short-circuit current, fill factor, power conversion efficiency, series and sheet resistance of inverted PCDTBT: PCBM solar cells fabricated with no insertion of cathode buffer interlayers.

ITO Treatment	$V_{oc}$ (V) ( $\pm 0.05$ )*		$J_{sc}$ (mA.cm <sup>-2</sup> )	FF (%)	PCE (%)	$R_s$ ( $\Omega$ .cm <sup>2</sup> )	$R_{sh}$ ( $\Omega$ .cm <sup>2</sup> )
	Average	Max					
<sup>a)</sup> 25° C	0.85	0.89	8.04	63.7	4.52	28.0	737
100° C	0.81	0.86	7.73	61.7	3.99	16.0	672
200° C	0.80	0.83	7.89	60.8	3.84	15.0	698
300° C	0.71	0.76	8.43	58.5	3.65	12.0	568
400° C	0.70	0.72	8.24	57.7	3.55	14.0	576
<sup>b)</sup> MoO <sub>3</sub> -Al	----	0.89	10.70	66.0	6.28	----	----
<sup>c)</sup> PFN	----	0.91	11.71	57.0	5.94	2.7	474
<sup>d)</sup> PCP-EP	----	0.88	08.76	56.9	5.48	6.7	597

\* The maximum standard deviation error of ten devices with four working pixels for each annealing condition.

<sup>a)</sup> Reference of inverted devices fabricated in our lab, onto non-annealed ITO substrates. Inverted devices have the structure of <sup>b)</sup> ITO/MoO<sub>3</sub>-Al/PCDTBT:PC<sub>70</sub>BM/MoO<sub>3</sub>/Al taken from Ref [33],

<sup>c)</sup> ITO/PFN/PCDTBT:PC<sub>70</sub>BM/MoO<sub>3</sub>/Ag taken from Ref [30],

and <sup>d)</sup> ITO/PCP-EP/PCDTBT:PC<sub>70</sub>BM/MoO<sub>3</sub>/Al taken from Ref [31].

The average and best device parameters as a function of annealing temperatures are summarized in Table I. The reference here is assigned to devices fabricated on un-annealed ITO substrates, so-called as 25°C. It can be seen that thermal annealing has a negative effect on device parameters except the short-circuit current. Therefore, the best performance was observed for devices fabricated at 25°C; 0.89 eV, 8.04 mA.cm<sup>-2</sup>, 63.68 %, and 4.52 % were obtained for  $V_{oc}$ ,  $J_{sc}$ , FF and PCE, respectively. Considering  $J_{sc}$ , a reduction of 4 % in the initial value was observed at low temperatures  $\leq 200^\circ$  C. For high temperatures ( $> 200^\circ$  C),  $J_{sc}$  was slightly improved by 5 %. This can be attributed to the changes in the series resistance ( $R_s$ ).  $R_s$  is reduced from 28.0  $\Omega$ .cm<sup>2</sup> at 25°C to 16.0  $\Omega$ .cm<sup>2</sup> at 100°C resulting in reduced  $J_{sc}$  from 8.04 to 7.73 mA.cm<sup>-2</sup>. A further reduction in  $R_s$  at 300°C ( $\approx 12.0 \Omega$ .cm<sup>2</sup>) increases  $J_{sc}$  up to 8.43 mA.cm<sup>-2</sup>. Despite of the slight enhancement in  $J_{sc}$  at high temperatures, the power conversion efficiency was not enhanced due to the significant reduction in the fill factor; FF of 58.5 % and PCE of 3.65 % were obtained at 300° C.

The  $V_{oc}$  of devices is gradually reduced upon thermal annealing with measured values of 0.86 V and 0.76 V for samples annealed at 100°C and 300°C, respectively. To understand the origin of  $V_{oc}$  reduction, we investigate the work function of blank ITO substrates. Figure 2(a) shows the changes in the low kinetic energy region of the UPS spectra. The WF of non-annealed ITO is found to be  $4.20 \pm 0.03$  eV. For ITO annealed at 100°C, the WF is slightly increased to  $4.28 \pm 0.03$  eV. A further increase to  $4.35 \pm 0.03$  eV and  $4.47 \pm 0.04$  eV is observed for 200°C and 300°C, respectively. However, an unexpected reduction in ITO work function of  $4.44 \pm 0.05$  eV is found when it was annealed at 400°C, suggesting different source of surface chemical reaction that will be discussed later on.

Furthermore, the electronic structure of ITO/PC<sub>70</sub>BM interface was investigated. For unannealed substrates, the HOMO edge of spin-coated PC<sub>70</sub>BM layer is located at  $1.74 \pm 0.02$  eV near the Fermi level as shown in Figure 2(b). This is deeper than the recent reported HOMO position by 0.12 eV applying similar approach [34], this may attribute to the different sources of PC<sub>70</sub>BM used. However, the HOMO edge of PC<sub>70</sub>BM is slightly lifted up to  $1.72 \pm 0.02$  eV when deposited onto ITO annealed at 100°C. When deposited onto ITO annealed at higher temperatures, the HOMO edge remains unaffected, suggesting there is negligible charge transfer between PCBM and ITO [35].

In Figure 2(c), the XPS spectra provides evidence of the chemical reaction undergone onto the surface of blank ITO. The peak position of O 1s core level that corresponds to In-O bond is at 529.78 eV for non-annealed ITO, which is in agreement with the literature [36][37]. There are negligible shifts in the binding energy ( $E_b$ ) with low temperatures, whereas shifts of 0.15 eV and 0.13 eV towards lower  $E_b$  are observed for 300°C and 400°C, respectively. These shifts associate with increased peak intensities and disappearance of the characteristic shoulder at 530.99 eV. The observed shoulders at lower energies are likely to be due to C-O and C=O containing species adsorbed onto the surface. High temperatures annealing effectively removes these species from the surface by breaking them down and being released as gas. The shift in the peak position at higher temperatures could be due to ITO reducing its oxidation states, creating metallic defect states and hence making the WF shallower.

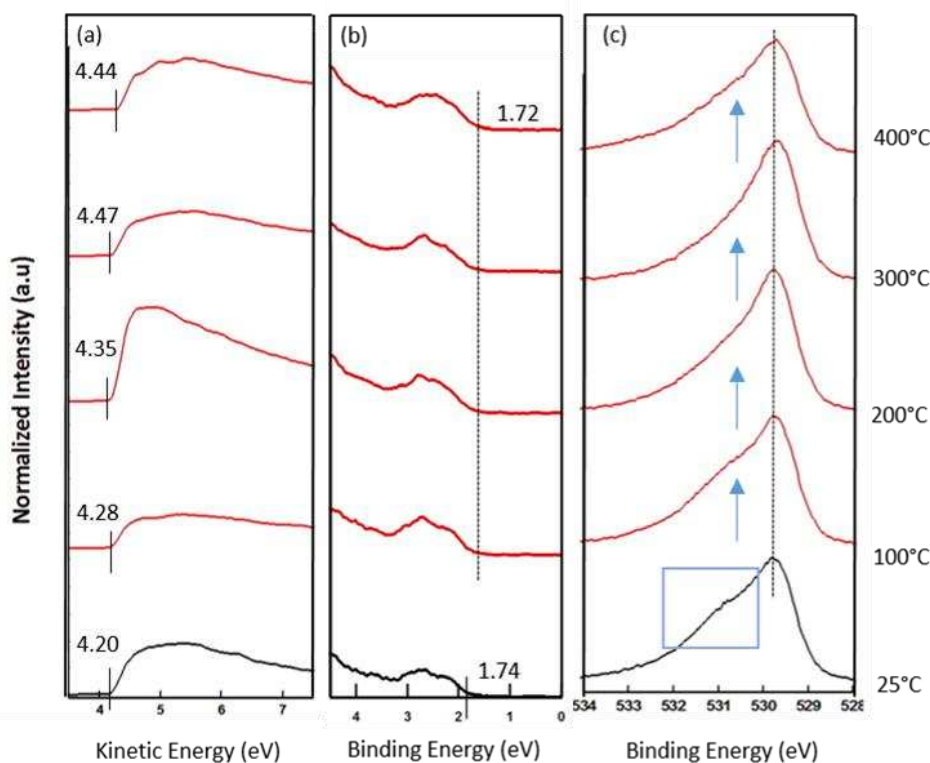


**FIG. 2.** UPS spectra (a) at the low kinetic energy region showing changes in the work function of blank ITO, (b) the corresponding valence band region near the Fermi level at ITO/PCBM interface during ITO thermal annealing. (c) XPS spectra of oxygen narrow scan (O 1s) for blank ITO as a function of thermal annealing.

The correlation between the open circuit voltages and substrate work function is examined. Care was taken to demonstrate the effect of cathode interfacial modification reported previously only for PCDTBT: PC<sub>70</sub>BM based inverted solar cells. The data is extracted from Ref [30][31][33]. In Figure 3, it can be seen that there are two distinguished features. First, the independence of  $V_{oc}$  on the WF. This is observed for work function values less than 4.30 eV. We have seen earlier that unannealed ITO devices were obtained an average  $V_{oc}$  of  $0.85 \pm 0.05$  eV (WF;  $4.20 \pm 0.03$  eV). Contrary, a maximum  $V_{oc}$  of 0.88 eV (WF; 4.30 eV), 0.89 eV (WF; 4.10 eV) and 0.90 eV (WF; 4.0 eV) were reported for modified ITO with PCP-EP [31], MoO<sub>3</sub>-Al [33] and PFN [30] thin layers, respectively. The second feature is the proportionality of  $V_{oc}$  with the WF. This is realized when ITO WF is higher than 4.30 eV. With respect to the high efficiencies obtained for modified ITO devices (see table I), their best  $V_{oc}$  falls within the range of errors calculated for our devices. This is true even for worse modified ITO devices. The threshold work function is, within error the same as the LUMO energy level of PC<sub>70</sub>BM.

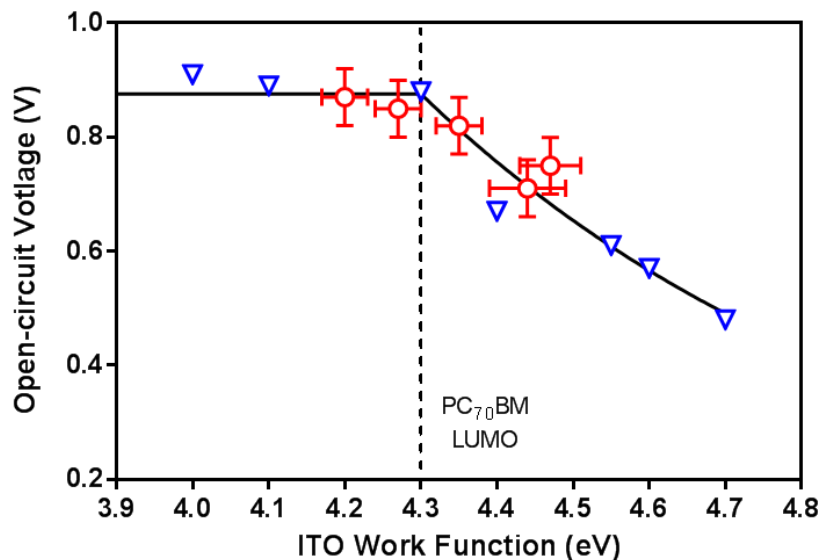


**FIG. 3.** Dependence of the open-circuit voltage on the substrate work function for inverted PCDTBT: PCBM solar cells fabricated on modified ITO electrodes with buffer interlayers (triangles) taken from Ref [30]-[31]-[33], and thermally annealed ITO electrodes without interfacial layer (circles) indicating our work. The solid line indicates the fitted curve. The dotted-vertical line indicates the LUMO energy level of PCBM.

#### 4. Conclusion

In Summary, the open circuit voltages of inverted polycarbazole: fullerene solar cells have been examined in terms of interfacial design. This is achieved by thermal annealing of blank ITO. The changes in ITO work function detected by UPS appear to correlate with the reduction observed in  $V_{oc}$  although our devices exhibit good JV curves. When compared to existing literature, a threshold work function that is equivalent to fullerene LUMO is seen, and



should be overcome to realize high  $V_{oc}$ . However, it is still not known whether a further reduction in substrate work function is required for the realization of the very highest  $V_{oc}$ .

## Acknowledgements

Rania Alqurashi thanks the Saudi Cultural Bureau in London, UK, and Al-Baha University, Saudi Arabia, for the provision of a PhD scholarship. She would also like to thank Dr. Deborah Hammond at Sheffield Surface Analysis Centre, Kroto Centre for High Resolution Images and Analysis, UK for the operation and maintenance of the UPS and XPS instruments. Access to the XPS instrument was funded through EPSRC grant EP/I032541/1.

## References

- [1] A. J. Heeger, "25th anniversary article: Bulk heterojunction solar cells: understanding the mechanism of operation," *Adv. Mater.*, vol. 26, no. 1, pp. 10–27, Jan. 2014.
- [2] S.-H. Liao, H.-J. Jhuo, P.-N. Yeh, Y.-S. Cheng, Y.-L. Li, Y.-H. Lee, S. Sharma, and S.-A. Chen, "Single Junction Inverted Polymer Solar Cell Reaching Power Conversion Efficiency 10.31% by Employing Dual-Doped Zinc Oxide Nano-Film as Cathode Interlayer," *Sci. Rep.*, vol. 4, p. 6813, Oct. 2014.
- [3] & A. J. H. Sung Heum Park, Anshuman Roy, Serge Beaupré, Shinuk Cho, Nelson Coates, Ji Sun Moon, Daniel Moses, Mario Leclerc, Kwanghee Lee, "Bulk heterojunction solar cells with internal quantum efficiency approaching 100%," *Nat. Photonics*, vol. 3, pp. 297–302, 2009.
- [4] M. Jørgensen, K. Norrman, and F. C. Krebs, "Stability/degradation of polymer solar cells," *Sol. Energy Mater. Sol. Cells*, vol. 92, no. 7, pp. 686–714, Jul. 2008.
- [5] Y. Liu, T. T. Larsen-Olsen, X. Zhao, B. Andreasen, R. R. Søndergaard, M. Helgesen, K. Norrman, M. Jørgensen, F. C. Krebs, X. Zhan, A. B. Liu, Yao, Larsen-Olsen. Thue T, Zhao. Xingang, and Z. X. Søndergaard. Roar R, Helgesen. Martin, Norrman. Kion, Jørgensen. Mikkel, Krebs. Frederik C, "All polymer photovoltaics: From small inverted devices to large roll-to-roll coated and printed solar cells," *Sol. Energy Mater. Sol. Cells*, vol. 112, pp. 157–162, May 2013.
- [6] B. Qi and J. Wang, "Open-circuit voltage in organic solar cells," *J. Mater. Chem.*, vol. 22, no. 46, p. 24315, 2012.
- [7] C. J. Brabec, A. Cravino, D. Meissner, N. S. Sariciftci, T. Fromherz, M. T. Rispens, L. Sanchez, and J. C. Hummelen, "Origin of the Open Circuit Voltage of Plastic Solar Cells," *Adv. Funct. Mater.*, vol. 11, no. 5, pp. 374–380, Oct. 2001.
- [8] C. M. Ramsdale, J. A. Barker, A. C. Arias, J. D. MacKenzie, R. H. Friend, and N. C. Greenham, "The origin of the open-circuit voltage in polyfluorene-based photovoltaic devices," *J. Appl. Phys.*, vol. 92, no. 8, p. 4266, Oct. 2002.
- [9] J. Liu, Y. Shi, and Y. Yang, "Solvation-Induced Morphology Effects on the Performance of Polymer-Based Photovoltaic Devices," *Adv. Funct. Mater.*, vol. 11, no. 6, p. 420, Dec. 2001.
- [10] S. E. Shaheen, C. J. Brabec, N. S. Sariciftci, F. Padinger, T. Fromherz, and J. C. Hummelen, "2.5% efficient organic plastic solar cells," *Appl. Phys. Lett.*, vol. 78, no. 6, p. 841, Feb. 2001.
- [11] A. Gadisa, M. Svensson, M. R. Andersson, and O. Inganäs, "Correlation between oxidation potential and open-circuit voltage of composite solar cells based on blends of polythiophenes/ fullerene derivative," *Appl. Phys.*



Lett., vol. 84, no. 9, p. 1609, Feb. 2004.

- [12] L. J. a Koster, V. D. Mihailetschi, R. Ramaker, and P. W. M. Blom, “Light intensity dependence of open-circuit voltage of polymer:fullerene solar cells,” *Appl. Phys. Lett.*, vol. 86, no. 12, pp. 1–3, 2005.
- [13] M. C. Scharber, D. Mühlbacher, M. Koppe, P. Denk, C. Waldauf, a. J. Heeger, and C. J. Brabec, “Design Rules for Donors in Bulk-Heterojunction Solar Cells—Towards 10 % Energy-Conversion Efficiency,” *Adv. Mater.*, vol. 18, no. 6, pp. 789–794, Mar. 2006.
- [14] V. D. Mihailetschi, P. W. M. Blom, J. C. Hummelen, and M. T. Rispens, “Cathode dependence of the open-circuit voltage of polymer:fullerene bulk heterojunction solar cells,” *J. Appl. Phys.*, vol. 94, no. 10, p. 6849, Oct. 2003.
- [15] J. C. Blakesley and N. C. Greenham, “Charge transfer at polymer-electrode interfaces: The effect of energetic disorder and thermal injection on band bending and open-circuit voltage,” *J. Appl. Phys.*, vol. 106, no. 3, p. 034507, Aug. 2009.
- [16] C. Tengstedt, W. Osikowicz, W. R. Salaneck, I. D. Parker, C.-H. Hsu, and M. Fahlman, “Fermi-level pinning at conjugated polymer interfaces,” *Appl. Phys. Lett.*, vol. 88, no. 5, p. 053502, Feb. 2006.
- [17] A. Crispin, X. Crispin, M. Fahlman, M. Berggren, and W. R. Salaneck, “Transition between energy level alignment regimes at a low band gap polymer-electrode interfaces,” *Appl. Phys. Lett.*, vol. 89, no. 21, p. 213503, Nov. 2006.
- [18] K. Vandewal, K. Tvingstedt, A. Gadisa, O. Inganäs, and J. V Manca, “Relating the open-circuit voltage to interface molecular properties of donor:acceptor bulk heterojunction solar cells,” *Phys. Rev. B*, vol. 81, p. 2452041, 2010.
- [19] T. M. Clarke, J. Peet, A. Nattestad, N. Drolet, G. Dennler, C. Lungenschmied, M. Leclerc, and A. J. Mozer, “Charge carrier mobility, bimolecular recombination and trapping in polycarbazole copolymer:fullerene (PCDTBT:PCBM) bulk heterojunction solar cells,” *Org. Electron.*, vol. 13, no. 11, pp. 2639–2646, Nov. 2012.
- [20] K. S. Nalwa, H. K. Kodali, B. Ganapathysubramanian, and S. Chaudhary, “Dependence of recombination mechanisms and strength on processing conditions in polymer solar cells,” *Appl. Phys. Lett.*, vol. 99, pp. 4–7, 2011.
- [21] K. Vandewal, K. Tvingstedt, A. Gadisa, O. Inganäs, and J. V Manca, “On the origin of the open-circuit voltage of polymer-fullerene solar cells,” *Nat. Mater.*, vol. 8, no. 11, pp. 904–909, 2009.
- [22] G. Garcia-Belmonte and J. Bisquert, “Open-circuit voltage limit caused by recombination through tail states in bulk heterojunction polymer-fullerene solar cells,” *Appl. Phys. Lett.*, vol. 96, no. 11, p. 113301, 2010.
- [23] V. D. Mihailetschi, L. J. A. Koster, and P. W. M. Blom, “Effect of metal electrodes on the performance of polymer:fullerene bulk heterojunction solar cells,” *Appl. Phys. Lett.*, vol. 85, no. 6, p. 970, Aug. 2004.
- [24] H. Jin, M. Tuomikoski, J. Hiltunen, P. Kopola, A. Maaninen, and F. Pino, “Polymer–Electrode Interfacial Effect on Photovoltaic Performances in Poly(3-hexylthiophene):Phenyl-C61-butyric Acid Methyl Ester Based Solar Cells,” *J. Phys. Chem. C*, vol. 113, no. 38, pp. 16807–16810, Sep. 2009.
- [25] A. Kumar, S. Sista, and Y. Yang, “Dipole induced anomalous S-shape I-V curves in polymer solar cells,” *J. Appl. Phys.*, vol. 105, no. 9, pp. 1–6, 2009.
- [26] K. Schulze, C. Uhrich, R. Schüppel, K. Leo, M. Pfeiffer, E. Brier, E. Reinold, and P. Bäuerle, “Efficient Vacuum-Deposited Organic Solar Cells Based on a New Low-Bandgap Oligothiophene and Fullerene C60,” *Adv. Mater.*, vol. 18, no. 21, pp. 2872–2875, 2006.
- [27] A. Wagenpfahl, D. Rauh, M. Binder, C. Deibel, and V. Dyakonov, “S-shaped current-voltage characteristics of organic solar devices,” *Phys. Rev. B*, vol. 82, no. 11, p. 115306, Sep. 2010.
- [28] Y. Yan and Y. Song, “Effect of PEI cathode interlayer on work function and interface resistance of ITO electrode in the inverted polymer solar cells,” *Org. Electron.*, vol. 17, pp. 94–101, 2015.
- [29] and K.-Y. Aiyuan Li, Riming Nie, Xianyu Deng, HuaixinWei, Shizhao Zheng, Yanqing Li, Jianxin Tang, “Highly efficient inverted organic solar cells using amino acid modified indium tin oxide as cathode,” *Appl. Phys. Lett.*, vol. 104, p. 123303, 2014.
- [30] R. Xia, D.-S. Leem, T. Kirchartz, S. Spencer, C. Murphy, Z. He, H. Wu, S. Su, Y. Cao, J. S. Kim, J. C. DeMello, D. D. C. Bradley, and J. Nelson, “Investigation of a Conjugated Polyelectrolyte Interlayer for Inverted Polymer:Fullerene Solar Cells,” *Adv. Energy Mater.*, vol. 3, no. 6, pp. 718–723, Jun. 2013.

- [31] Y. Zhu, X. Xu, L. Zhang, J. Chen, and Y. Cao, "High efficiency inverted polymeric bulk-heterojunction solar cells with hydrophilic conjugated polymers as cathode interlayer on ITO," *Sol. Energy Mater. Sol. Cells*, vol. 97, pp. 83–88, Feb. 2012.
- [32] M. Bhatti, A. Rana, and A. Khan, 'Characterization of rf-sputtered indium tin oxide thin films', *Mater Chem and Phys*, vol 84, pp. 126-130, Apr. 2004.
- [33] J. Liu, S. Shao, G. Fang, B. Meng, Z. Xie, and L. Wang, "High-Efficiency Inverted Polymer Solar Cells with Transparent and Work-Function Tunable MoO<sub>3</sub>-Al Composite Film as Cathode Buffer Layer," *Adv. Mater.*, vol. 24, no. 20, pp. 2774–2779, May 2012.
- [34] R. Nakanishi, A. Nogimura, R. Eguchi, and K. Kanai, "Electronic structure of fullerene derivatives in organic photovoltaics," *Org. Electron.*, vol. 15, no. 11, pp. 2912–2921, Nov. 2014.
- [35] S. Zhong, R. Wang, H. Ying Mao, Z. He, H. Wu, W. Chen, and Y. Cao, "Interface investigation of the alcohol-/water-soluble conjugated polymer PFN as cathode interfacial layer in organic solar cells," *J. Appl. Phys.*, vol. 114, no. 11, p. 113709, Sep. 2013.
- [36] C. Donley, D. Dunphy, D. Paine, C. Carter, K. Nebesny, P. Lee, D. Alloway, and N. R. Armstrong, "Characterization of Indium–Tin Oxide Interfaces Using X-ray Photoelectron Spectroscopy and Redox Processes of a Chemisorbed Probe Molecule: Effect of Surface Pretreatment Conditions," *Langmuir*, vol. 18, no. 2, pp. 450–457, Jan. 2002.
- [37] K. H. Lee, H. W. Jang, K. B. Kim, Y. H. Tak, and J. L. Lee, "Mechanism for the increase of indium-tin-oxide work function by O<sub>2</sub> inductively coupled plasma treatment," *J. Appl. Phys.*, vol. 95, no. 2004, pp. 586–590, 2004.